Biology of Reproduction, 2022, **107(6)**, 1439–1451
https://doi.org/10.1093/biolre/ioac180
Advance access publication date 20 September 2022
Research Article

PMCA1 depletion in mouse eggs amplifies calcium signaling and impacts offspring growth†

Virginia Savy[1], Paula Stein[1], Min Shi[2] and Carmen J. Williams[1,*]

[1]Reproductive & Developmental Biology Laboratory, National Institute of Environmental Health Sciences, National Institutes of Health, Research Triangle Park, NC, USA
[2]Biostatistics & Computational Biology Branch, National Institute of Environmental Health Sciences, National Institutes of Health, Research Triangle Park, NC, USA

***Correspondence:** 111 TW Alexander Dr, Research Triangle Park, NC 27709, USA. E-mail: williamsc5@niehs.nih.gov

†**Grant support:** This work was supported by the Intramural Research Program of the National Institutes of Health, National Institute of Environmental Health Sciences, 1ZIAES102985.

Abstract

Egg activation in mammals is triggered by oscillations in egg intracellular calcium (Ca^{2+}) level. Ca^{2+} oscillation patterns can be modified in vitro by changing the ionic composition of culture media or in vivo by conditions affecting mitochondrial function, such as obesity and inflammation. In mice, disruption of Ca^{2+} oscillations in vitro impacts embryo development and offspring growth. Here we tested the hypothesis that, even without in vitro manipulation, abnormal Ca^{2+} signaling following fertilization impacts offspring growth. Plasma membrane Ca^{2+} ATPases (PMCA) extrude cytosolic Ca^{2+} to restore Ca^{2+} homeostasis. To disrupt Ca^{2+} signaling in vivo, we conditionally deleted PMCA1 (cKO) in oocytes. As anticipated, in vitro fertilized cKO eggs had increased Ca^{2+} exposure relative to controls. To assess the impact on offspring growth, cKO females were mated to wild type males to generate pups that had high Ca^{2+} exposure at fertilization. Because these offspring would be heterozygous, we also tested the impact of global PMCA1 heterozygosity on offspring growth. Control heterozygous pups that had normal Ca^{2+} at fertilization were generated by mating wild type females to heterozygous males; these control offspring weighed significantly less than their wild type siblings. However, heterozygous offspring from cKO eggs (and high Ca^{2+} exposure) were larger than heterozygous controls at 12 week-of-age and males had altered body composition. Our results show that global PMCA1 haploinsufficiency impacts growth and support that abnormal Ca^{2+} signaling after fertilization in vivo has a long-term impact on offspring weight. These findings are relevant for environmental and medical conditions affecting Ca^{2+} handling and for design of culture conditions and procedures for domestic animal and human assisted reproduction.

Summary Sentence
Plasma membrane calcium ATPase 1 (PMCA1) in eggs regulates calcium homeostasis at fertilization, and offspring derived from PMCA1-null eggs (and excess calcium signal at fertilization) weigh more than controls with normal calcium.

Graphical Abstract

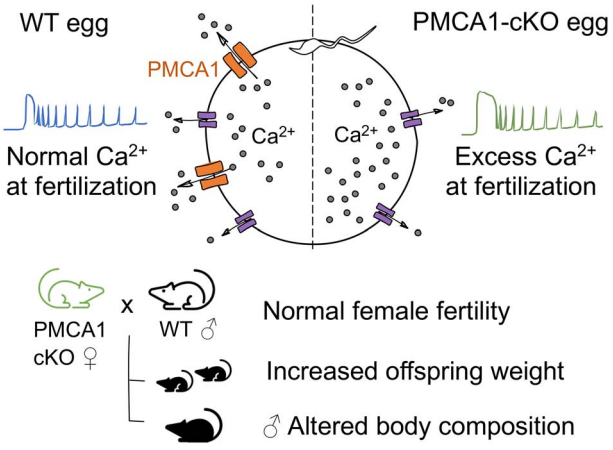

Keywords: PMCA1, calcium, egg activation, DOHaD, fertilization

Received: July 12, 2022. **Revised:** August 19, 2022. **Accepted:** September 19, 2022

Introduction

The cascade of events that transform an egg into an embryo, known as "egg activation" events, is initiated by a dramatic yet transient increase in the egg's intracellular calcium (Ca^{2+}) level. Ca^{2+}-mediated egg activation is conserved across the animal kingdom, but Ca^{2+} signal dynamics vary extensively. In mammals, Ca^{2+} dynamics take the form of multiple transient increases in cytoplasmic Ca^{2+}, or Ca^{2+} oscillations. Based on in vitro studies, Ca^{2+} oscillations orchestrate the specialized events of egg activation in a temporally progressive manner. For example, early egg activation events such as cortical granule exocytosis and cell cycle resumption require few Ca^{2+} oscillations, but late events such as pronucleus formation require more Ca^{2+} oscillations [1]. These Ca^{2+} signals are translated into biochemical information in part by activating Ca^{2+}/calmodulin-dependent protein kinase II (CaMKII) gamma, which is the major downstream mediator of egg activation [2–4]. Progression of egg activation appears to depend on the total Ca^{2+} signal over time, which results from the combined attributes of amplitude, frequency, duration, and persistence of Ca^{2+} oscillations [1, 5], although additional information encoded in the Ca^{2+} oscillatory pattern cannot be ruled out. There is also no information available regarding how much or how little Ca^{2+} signal is needed for egg activation in vivo.

In mice, experimental modulation of Ca^{2+} oscillations in early one-cell (1C) embryos following in vivo fertilization impacts embryo development and offspring growth. One-cell embryos artificially exposed to either suboptimal Ca^{2+} or excess Ca^{2+} have reduced developmental competence; the exact phenotype depends on the direction in which Ca^{2+} is altered [6]. Premature termination of Ca^{2+} signals negatively affects implantation rate, whereas Ca^{2+} hyperstimulation results in normal implantation but suboptimal postimplantation development. Moreover, embryos exposed to excess Ca^{2+} have, after birth, transient yet significant alterations in body weight during development. Similarly, experimental alterations in Ca^{2+} oscillatory patterns induced by changing the ionic composition of embryo culture medium are associated with differences in offspring metabolic parameters [7]. These studies demonstrate that information encoded in fertilization-induced Ca^{2+} oscillations persists and impacts offspring physiology. However, all of these experiments were performed by in vitro manipulation of early embryos followed by embryo transfer, and numerous studies have documented that in vitro manipulation alone is sufficient to affect offspring outcomes [8–11]. Therefore, it remains unclear whether these findings are caused by the Ca^{2+} alterations alone or by the combined effects of Ca^{2+} alterations and in vitro manipulation.

As in somatic cells, Ca^{2+} signaling during mammalian fertilization is regulated by modulators of Ca^{2+} storage, release, and reuptake. Ca^{2+} accumulates during oocyte maturation and is stored mainly in the endoplasmic reticulum (ER). At fertilization, Ca^{2+} oscillations are triggered following sperm-egg fusion by sperm-specific phospholipase C zeta (PLCζ). PLCζ mediates the production of inositol 1,4,5-trisphosphate (IP3), which binds the IP3 receptor and causes Ca^{2+} release from the ER into the egg cytosol and raises the cytosolic Ca^{2+} level from a basal level of ~100 nM to the low μM range [12]. To restore cytosolic Ca^{2+} to basal levels, sarco/endoplasmic reticulum Ca^{2+}-ATPases (SERCA) pump Ca^{2+} back into the ER. Although it has not yet been documented experimentally in mammalian eggs, it is likely that as in somatic cells, plasma membrane Ca^{2+} ATPases (PMCA) clear excess Ca^{2+} by moving it across the plasma membrane to the extracellular milieu (Ca^{2+} efflux), resulting in a net loss of Ca^{2+} from the egg. Ca^{2+} oscillations only continue if ER Ca^{2+} stores are refilled with extracellular Ca^{2+} that enters the egg through plasma membrane Ca^{2+} channels [13–16]. Overall, although Ca^{2+} oscillations are triggered by sperm PLCζ, Ca^{2+} modulators in the mature egg are crucial for shaping Ca^{2+} dynamics and, therefore, to provide the appropriate developmental information encoded within the Ca^{2+} signature.

Expression and function of PMCAs in mammalian eggs are not yet characterized. In Xenopus oocytes, there is at least one PMCA based on immunodetection [17]. In mouse eggs, "Ca^{2+} insulation" using high concentrations of gadolinium in the extracellular medium, which in somatic cells blocks PMCA function, prolongs the duration of the first Ca^{2+} transient following fertilization by intracytoplasmic sperm injection [18, 19]. These findings suggest that at least one PMCA isoform is present and functional in mouse eggs. There are four mammalian isoforms of PMCA, encoded by the gene family *Atp2b*. PMCA1 and PMCA4 are ubiquitously expressed [20, 21]. PMCA2 is mainly expressed in the nervous system and mammary gland, whereas PMCA3 is restricted to the nervous system in adult mice [22]. Global deletion of PMCA1 results in an embryonic lethal phenotype [20]. Moreover, PMCA1 is regulated by CaMKII, which is the main downstream effector of Ca^{2+} at fertilization, and has a higher affinity for ATP than other isoforms. These findings led us to speculate that eggs lacking PMCA1 would have abnormally long duration Ca^{2+} transients after fertilization.

Here we tested the hypothesis that PMCA1 regulates Ca^{2+} homeostasis at fertilization and that the resulting changes in Ca^{2+} oscillatory dynamics in vivo impact offspring postnatal growth and health. Oocyte-specific PMCA1 conditional knockout (cKO) mice were generated by crossing the Zp3-cre transgene into an *Atp2b1*-floxed mouse line. Our key findings were that PMCA1 is required to limit the length of each sperm-induced Ca^{2+} transient, that global PMCA1 haploinsufficiency reduces offspring weight, and that offspring generated from eggs exposed to increased Ca^{2+} signal at fertilization have increased weight and altered body composition. Our results reveal the importance of PMCA1 in maintaining Ca^{2+} homeostasis at fertilization and demonstrate that even without in vitro manipulation, abnormal Ca^{2+} signaling at fertilization has a long-term impact on offspring growth.

Methods

Mice

CF-1 females (Hsd:NSA(CF-1)) were purchased from Envigo (Indianapolis, IN, USA) and used for gamete and embryo collection for the developmental gene expression profile. FVB/NJ mice (Strain #001800) were purchased from Jackson Laboratory (Bar Harbor, ME, USA) and intercrossed to obtain pups used for litter size standardization. Zp3-cre males (Strain #003651; [23]) and C57BL/6J males (Strain #000664) used for breeding were obtained from Jackson Laboratory (Bar Harbor). All animal procedures complied with NIH/NIEHS animal care guidelines.

To generate oocyte-specific *Atp2b1* knockout mice, we used JM8A3.N1 embryonic stem cells carrying a floxed allele of *Atp2b1* (RRID:MMRRC_052502-UCD; Wellcome Trust Sanger Institute and Knockout Mouse Project Repository [24]). These ES cells carried a promoter-driven selection cassette (FRT-LacZ-Neo-FRT) and a loxP site between exons 1 and 2 of the *Atp2b1* gene and a second loxP sequence between exons 2 and 3. Chimeric founders were generated by blastocyst microinjection and embryo transfer. Following germ-line transmission, female offspring (B6;Cg-Atp2b1 < tm1a(KOMP)Wtsi>) were mated to CAG-FLPe males (B6-Tg(ACTB-Flpe)<2Arte > N10; Taconic Biosciences, Hudson, NY) to remove the selection cassette and generate *Atp2b1*-floxed mice [B6;Cg-Atp2b1 < tm1c (KOMP)Wtsi>]. These mice were bred to Zp3-cre males, then intercrossed to generate homozygous *Atp2b1*-floxed (*Atp2b1*-f/f) offspring with or without Zp3-cre. *Atp2b1*-f/f females were mated to *Atp2b1*-ff;Zp3-cre males to generate *Atp2b1*-f/f (Ctrl) or *Atp2b1*-f/f;Zp3-cre (cKO) females.

Gamete collection

Gamete collection was performed as previously described [16]. Briefly, germinal vesicle (GV) stage oocytes were obtained from 6–12-week-old females, 44–48 h after injection with 7.5 IU of equine chorionic gonadotropin (eCG, Lee Biosolutions, Maryland Heights, MO). Minimal Essential Medium (MEM) with Hepes (Thermo Fisher, Waltham, MA) containing 0.1% polyvinyl alcohol (PVA) and 2.5 μM milrinone (both from Sigma, St. Louis, MO) was used to maintain meiotic arrest. Oocytes with a visible GV were cultured under oil in drops of MEM-alpha (Thermo Fisher) containing 5% FBS (Atlanta Biologicals) and milrinone in a humidified atmosphere of 37°C and 5% CO_2. Metaphase II-arrested (MII) eggs were recovered from the oviducts of superovulated 6–12-week-old females. Superovulation consisted of 7.5 IU eCG, followed 48 h later by 7.5 IU human chorionic gonadotropin (hCG; Sigma). MII eggs were collected in MEM with Hepes, 0.1% PVA, and 0.1% hyaluronidase (Sigma) for removal of cumulus cells.

Growing, meiotically incompetent oocytes were recovered from 12 to 13-day-old CF-1 females after enzymatic digestion of ovarian tissue with 1 mg/ml collagenase (Worthington Biochemical Corp., Lakewood, NJ) and 2 mg/ml DNase I (Sigma). Embryos were obtained from adult CF-1 females previously superovulated and mated to 2–12-month-old B6SJLF1/J males. Embryos were flushed from oviducts and/or uteri at 16–20, 44, 68 and 96 h post-hCG, to obtain 1-cell (1C), 2-cell (2C), 8-cell (8C) and blastocyst stage embryos, respectively. Fifty oocytes/embryos were pooled together and stored at −80°C until use.

In vitro fertilization (IVF) and ratiometric Ca^{2+} imaging

MII eggs were pooled and treated with acid Tyrodes to remove the zona pellucidae. Following a 30-min recovery period, zona-free eggs were loaded with the Ca^{2+} indicator Fura-2 LR/AM (5 μM; Thermo Fisher) for 30 min in KSOM (Millipore Sigma) containing 0.02% pluronic F-127 (Thermo Fisher). Ctrl and cKO eggs were adhered side-by-side to glass-bottom dishes (MatTek, Ashland, MA) coated with Cell-Tak (Millipore Sigma) in a 150 μl drop of KSOM without BSA. After addition of 45 μl of human tubal fluid medium (HTF; Millipore Sigma) containing 4 mg/ml of AlbuMax I lipid-rich BSA (Life Technologies) (HTF–BSA), the media drops were covered with oil and placed on an environmentally controlled microscope stage (humidified atmosphere, 37°C and 5% CO_2).

For sperm isolation, the epididymides of an adult B6SJLF1/J male were placed into a 500 μl drop of HTF–BSA covered with mineral oil and cut several times. The dish was placed in the incubator for 15 min at 37°C and 5% CO_2 to allow the sperm to swim out. Then, the swim-up method was used to isolate motile sperm, as previously described [15].

Intracellular Ca^{2+} imaging was performed as previously described [15]. Briefly, 3–5 min after imaging was started, 5 μl of HTF–BSA containing 4×10^5 sperm/ml were added to the IVF dish to achieve a final concentration of 1×10^4 sperm/ml. Changes in the egg's intracellular Ca^{2+} level were monitored using a Hamamatsu ORCA-Flash 4.0 LT+ digital camera (Hamamatsu, Bridgewater, NJ) mounted on a Nikon Ti inverted microscope with a Nikon S Fluor 20×/0.75 NA objective (Nikon Instruments, Melville, NY) with excitation at 340 and 380 nM using a Lambda 10-B Optical Filter Changer (Sutter Instruments) and expressed as a fluorescence ratio (F340/F380).

Analysis of Ca^{2+} imaging data was done using custom R functions [25]. Briefly, for each trace, a custom function was used to estimate up points (Ca^{2+} rise) and down points (return to baseline). Then, non-peak data were used to estimate the baseline and the height of each oscillation and calculate the mid point as (baseline+peak height/2). Using this information, data were re-analyzed to determine the corrected baseline, amplitude, and number of oscillations. The area under the curve (AUC) was calculated by integration of peaks within 60 min from the first transient (first rise). Detailed information regarding the R functions can be found at (https://www.niehs.nih.gov/research/atniehs/labs/assets/docs/q_z/savy_rscript.zip).

ER Ca^{2+} store assay

Fura-2 LR-loaded eggs were adhered side-by-side to glass-bottom dishes (MatTek, Ashland, MA) containing 1800 μl of Ca^{2+} and magnesium-free CZB (CMF-CZB) without BSA [26]. The dishes were placed on the environmentally controlled microscope stage and baseline ratiometric imaging was performed for 3–5 min. Either thapsigargin (TG) (T7459; Life Technologies) or ionomycin (I0634; Sigma) was added in 200 μl of CMF-CZB to a final concentration of 10 μM or 5 μM, respectively. Intracellular Ca^{2+} imaging was performed as described for IVF.

RNA isolation and reverse transcription (RT)-quantitative PCR (qPCR)

Total RNA was isolated from matched sets of 18–20 full grown GV oocytes each from Ctrl or cKO females using an Arcturus PicoPure RNA Isolation kit (Life Technologies). RT and amplification were performed as previously described [27]. For qPCR, one oocyte equivalent of complementary DNA was used in each reaction and the ΔΔCT method [28] was used to compare the relative expression between groups, after *Gapdh* normalization. Primer sequences are provided (see Supplementary Table S1). For the *Atp2b1* and *Atp2b3* developmental gene expression profile, all samples were spiked with 1 ng of cRNA encoding enhanced green

fluorescent protein (EGFP) before RNA isolation. RT and amplification were performed as previously described [27]. Samples were analyzed by the ΔΔCT method [28] after *EGFP* normalization.

Offspring genotypes and growth trajectory

The growth trajectories of three groups of offspring were assessed. cKO (*Atb2b1*-f/f;Zp3-Cre) females were mated to wild type (WT) males to obtain heterozygous (*Atp2b1*+/−) offspring exposed to high Ca^{2+} at fertilization. WT females were mated to heterozygous (*Atp2b1*+/−) males to obtain *Atp2b1*+/+ (WT) and *Atp2b1*+/− (HET) siblings that were exposed to normal Ca^{2+} at fertilization. These mice were included to assess whether global PMCA1 haploinsufficiency affects offspring growth.

Only animals derived from litters with four pups or more were used in this study. Litter size was standardized at birth to eight pups, usually four of each sex, using 1–2-day-old FVB pups. Litter size before standardization was not different between groups (Supplementary Figure S1). Mice were weighed at birth and then weekly for 8 weeks. Pups were weaned at 3 weeks of age and fed with NIH-31 Rodent Diet. Starting at 4 weeks of age, pups were fed RD Western High Fat diet (Research Diets Inc., catalog # D12079Bi) ad libitum with free access to water until 3 months of age, when animals were returned to the NIH-31 Rodent Diet. Weight measurements were performed again at 12 weeks of age.

Glucose and insulin tolerance tests

Two females and two males/dam/group were assessed for glucose (GTT) and insulin (ITT) tolerance at 4 months of age. Mice were fasted overnight, with ad libitum access to water. After fasting, mice were weighed to determine the proper amount of glucose and insulin to be administered. Mice were placed in a restraining device for 5–10 s to snip the tail tip using a sharp blade. Basal blood glucose levels were determined using a Nova Max® Plus glucometer (Nova Biomedical, Waltham, MA). For GTT, 2 mg D-glucose/g body weight (Mallinckrodt Baker, Germany) was administered by i.p. injection. Mice were placed back in their cages and blood samples were collected for plasma glucose measurement at 15, 30, 45, 60, 90, 120, and 150 min after the injection, from the lifted tail of the mouse. For ITT, 0.75 IU insulin/g body weight (Humulin®-R U100, Lilly USA, IN) was injected i.p. and plasma glucose was determined at 15, 30, 45, 60, 75, 90, 120, and 180 min after the injection. Mice showing clinical signs of hypoglycemia during ITT were injected i.p. with 0.25 ml/20 grams of glucose solution and removed from the assay; <10% of the mice were removed. When possible, different animals were assessed for GTT and ITT. Otherwise, mice were allowed to recover for 2 weeks before performing ITT.

Body composition and femur length analysis

Body composition, including fat, lean and fluid content, was determined using a Bruker LF90 minispec (Bruker Optics, Inc., Billerica, MA). A daily quality control check was performed before the measurements using a standard provided by the manufacturer. Mice were weighed and placed in a restraint cylinder. The restrainer was lowered into the nuclear magnetic resonance system and measurements recorded using the minispec plus NF software.

Heterozygous offspring obtained from WT or cKO females were euthanized after 12 month of age. The right femur of each mouse was excised and incubated for 1 h at 60°C in 0.2 M NaOH for soft tissue digestion. Femurs were imaged using a Faxitron X-ray system (Faxitron Bioptics Ultrafocus DXA) and total femur length (mm) from the greater trochanter to the medial condyle was measured using BiopticsVision software.

Table 1. PMCA transcript abundance in GV oocytes

Gene	Calcium pump	Mean Ct	SEM
Atp2b1	PMCA1	30.32	0.12
Atp2b2	PMCA2	35.76	0.82
Atp2b3	PMCA3	28.20	0.39
Atp2b4	PMCA4	nd	-

Ct, threshold cycle; SEM, standard error of the mean; nd, not detected.

Statistics

Statistical analysis was performed using GraphPad Prism, version 9.0.2. Normally distributed data were analyzed with two-tailed *t* tests, whereas Mann–Whitney tests were used for non-parametric data. Data sets containing more than two groups were analyzed using ANOVA or Kruskal–Wallis tests for normally distributed or non-parametric data, respectively.

GTT and ITT data from male and female mice were analyzed separately. Linear mixed models were used with random intercept for animal ID nested within cage ID. The fixed effect terms included time as a categorical variable, experimental group, and their interactions. Heterogenous residual variances were allowed across the different time points. We tested differences between the two groups across different time points and adjusted *P*-values with Šidák correction.

Results

Atp2b1 is highly expressed in oocytes but is not essential for female fertility

To explore whether PMCA isoforms are expressed in the mouse oocyte and embryo, the mRNA levels of the different isoforms were measured by RT-qPCR. *Atp2b1*, *Atp2b2*, and *Atp2b3* mRNAs were present in GV oocytes but *Atp2b4* was undetectable (Table 1). Moreover, *Atp2b1* and *Atp2b3* were highly expressed relative to *Atp2b2*, assuming similar primer efficiency. *Atp2b1* and *Atp2b3* shared similar expression profiles across the different developmental stages, from growing oocyte (GO) to the blastocyst stage (Figure 1A and B). mRNA levels increased from GO to GV stage and remained high until the 2C stage. Transcript levels of both *Atp2b1* and *Atp2b3* were barely detectable between the 2C and 8C stages. However, by the blastocyst stage, *Atp2b1* relative abundance increased, whereas *Atp2b3* levels remained barely detectable. Based on these results, both PMCA1 and PMCA3 could play an important role during fertilization and/or early embryo development.

Proteins critical for fertilization and early embryo development are often encoded by maternal mRNAs whose translation markedly increases during oocyte maturation [29]. A hallmark of such maternal mRNAs is the presence of cytoplasmic polyadenylation elements (CPEs) in the 3′-untranslated region (3′ UTR). Seven CPEs were present upstream from the polyadenylation signal in the *Atp2b1* 3′UTR (GenBank Accession No. NM_026482.2). In contrast, there were no CPEs in the *Atp2b3* 3′UTR (GenBank Accession No. NM_177236.4). Moreover, although the only phenotype detected in

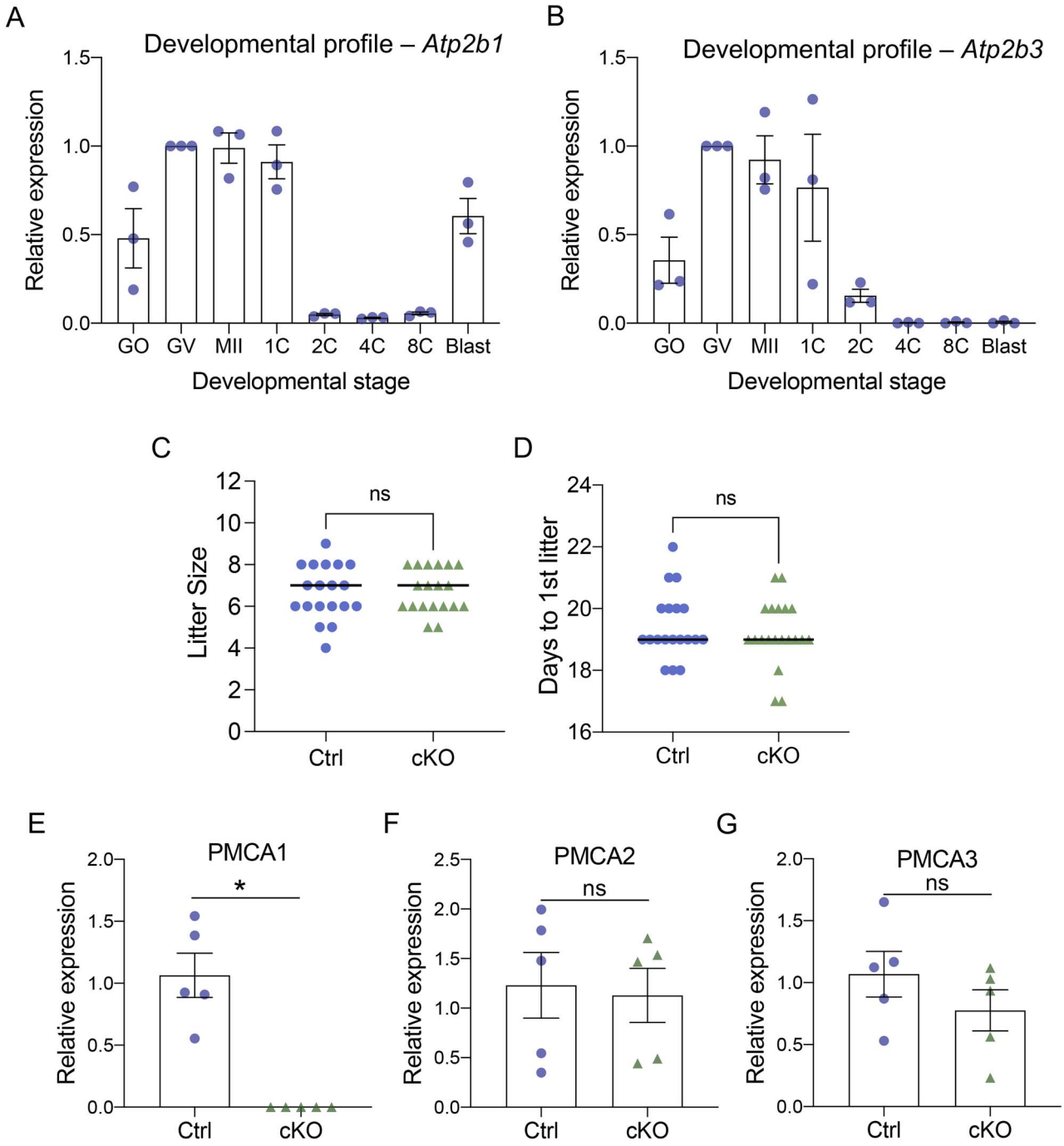

Figure 1. *Atp2b1* is highly expressed in oocytes but not essential for female fertility. (A–B) Developmental profile of *Atp2b1* and *Atp2b3* expression normalized to that in GV stage as mean +/− SEM. Each dot represents one biological replicate with 50 oocytes or embryos. GO, growing oocyte; GV, germinal vesicle stage oocyte; MII, metaphase II egg; 1C, 2C, 4C, 8C: 1-cell, 2-cell, 4-cell, 8-cell embryos; Blast, blastocyst. (C–D) Fertility assessment of control and cKO females mated to WT males; each dot represents one female. (C) Dot plot of live pups per litter and (D) days to first litter after mating. ns, not significant; Mann–Whitney test. (E–G) Expression of PMCA isoforms in control (Ctrl) and cKO oocytes. Each dot represents one biological replicate from matched sets of 18–20 full grown GV oocytes. Statistical analysis was done by Mann–Whitney test.

Atp2b3-null mice is a sleep disorder [30], the *Atp2b1*-null mice have an embryonic lethal phenotype [20]. These observations suggested that, unlike *Atp2b3*, *Atp2b1* is likely to play a role during fertilization or early embryo development. Unfortunately, despite testing multiple antibodies, the lack of a suitable antibody against PMCA1 hindered any attempt to assess the protein by immunofluorescence. Nevertheless, these findings led us to focus on *Atp2b1* for further analysis.

To determine the potential role of maternal PMCA1 in fertility, cKO (*Atp2b1*-f/f;Zp3-cre) and Ctrl (*Atp2b1*-f/f) females were mated to WT C57BL/6J males. No difference in the litter size or time to first litter was found between groups (Figure 1C and D). To determine whether the role of PMCA1 was masked by compensatory upregulation of other PMCA isoforms, the relative abundance of all *Atp2b* isoforms was assessed by RT-qPCR in cKO and Ctrl oocytes. As expected,

cKO GV oocytes lacked *Atp2b1* transcripts (Figure 1E). *Atp2b2* and *Atp2b3* mRNA abundance was comparable between control and cKO GV oocytes (Figure 1F and G). *Atp2b4* mRNA was not detectable either in cKO or Ctrl oocytes. Altogether, these results indicate that PMCA1 is not essential for female fertility and that loss of the *Atp2b1* isoform does not lead to compensatory upregulation of alternative isoforms.

Atp2b1 cKO eggs show aberrant Ca^{2+} responses at fertilization

To determine the functional presence and role of PMCA1 in mediating Ca^{2+} homeostasis at fertilization, MII eggs obtained from cKO and Ctrl females were in vitro fertilized while monitoring intracellular Ca^{2+} levels. Several parameters of Ca^{2+} dynamics, including length of the first transient, AUC of Ca^{2+} signal, and oscillation frequency were compared between groups. Differences in Ca^{2+} behavior between cKO and Ctrl eggs were evident, confirming at a functional level that the cKO strategy had worked well. The first Ca^{2+} transient was ~3 times longer in cKO eggs than controls (Figure 2A and B). Although the number of oscillations was not different, the total AUC of Ca^{2+} peaks in 60 min indicated that cKO eggs had ~65% more Ca^{2+} signal than controls (Figure 2C and D). The increased Ca^{2+} signal was not due exclusively to the increased length of the first transient, as the AUC excluding the first transient was also increased in cKO eggs, suggesting that each subsequent transient was also longer (Figure 2E).

To determine if *Atp2b1* heterozygosity led to haploinsufficiency in the Ca^{2+} response, WT females were mated to *Atp2b1*+/− (heterozygous) males to generate heterozygous and WT female siblings. The first Ca^{2+} transient was on average 1.5 times longer in eggs from heterozygous females than in WT eggs from siblings and was more variable (Figure 2F and G). However, no differences were found in any of the other parameters analyzed, including the total AUC, which indicates the accumulated level of Ca^{2+} exposure during fertilization (Figure 2H, I, and J). These results indicate that eggs from heterozygous females had only a mild abnormality in the Ca^{2+} response at fertilization during the first hour. Altogether, the abnormal Ca^{2+} dynamics observed at fertilization in cKO eggs, together with the haploinsufficient phenotype exhibited by eggs from heterozygous females, confirmed that MII eggs normally express a functional PMCA1 pump that regulates Ca^{2+} dynamics during fertilization.

Atp2b1 cKO eggs have increased internal Ca^{2+} stores

The length of the first Ca^{2+} transient is generally thought to reflect the amount of Ca^{2+} stored in the ER, but this parameter is also influenced by modulators of Ca^{2+} reuptake and Ca^{2+} efflux. The finding that the length of the first transient was longer in cKO and heterozygote-derived eggs compared with their controls suggested the possibility that lack of PMCA1 results in larger Ca^{2+} stores. A common assay for ER Ca^{2+} stores is treatment of cells with TG, an inhibitor of Ca^{2+} reuptake [31], which results in Ca^{2+} leak from the ER in proportion to the total amount of ER Ca^{2+}. TG treatment caused ~30% more Ca^{2+} release from cKO eggs than control eggs, based on measurement of the AUC (Figure 3A and B). However, AUC depends on both Ca^{2+} release from the ER and Ca^{2+} clearance from the cytoplasm, and we expected that the cytoplasmic clearance rate was lower in cKO than control eggs because cKO eggs lacked PMCA1, a major Ca^{2+} efflux pump. For this reason, we also assayed total internal Ca^{2+} stores using the Ca^{2+} ionophore, ionomycin. Ionomycin rapidly releases Ca^{2+} from all internal cellular stores, of which the ER is the major store, and the measurement of the Ca^{2+} peak immediately following treatment should reflect Ca^{2+} stores independent of the cytoplasmic Ca^{2+} efflux rate. Using this assay, we found that cKO eggs had ~16% more stored Ca^{2+} than controls (Figure 3C and D). We next tested whether eggs from heterozygous females (HET eggs) had altered Ca^{2+} stores. A 16% increase in TG-induced Ca^{2+} release was found in HET eggs relative to WT eggs from sibling controls (Figure 3E and F). Moreover, the ionomycin assay revealed that HET eggs had 7% more internal Ca^{2+} than WT eggs (Figure 3G and H), supporting the idea that HET eggs are haploinsufficient. These results indicate that lack of PMCA1 causes slightly increased internal Ca^{2+} store content and highlight the role of PMCA1 in maintaining Ca^{2+} homeostasis in the MII egg.

Increased Ca^{2+} at fertilization has long-term effects on offspring growth

Experimental modulation of Ca^{2+} levels following fertilization impacts embryo development and offspring growth [6]. However, it is possible that the in vitro manipulations utilized in this study sensitize the eggs to the effects of abnormal Ca^{2+} exposure, such as by increasing exposure to reactive oxygen species or altering embryo metabolism. We used the PMCA1 cKO mouse line to determine whether increased Ca^{2+} exposure without in vitro manipulation impacts offspring growth and metabolic parameters. This strategy makes the assumption that Ca^{2+} dynamics at fertilization in vivo are relatively similar to the dynamics observed in vitro for cKO and control eggs. cKO females were mated to WT males to generate pups that had high Ca^{2+} exposure at fertilization. Because these offspring were heterozygous (*Atp2b1*+/−), control heterozygous pups that had normal Ca^{2+} at fertilization were generated by mating WT females to heterozygous males. WT littermates obtained from these matings served as WT controls.

Interestingly, heterozygous controls were smaller than their WT siblings after weaning even though all mice were derived from WT eggs (Figure 4A and B). Comparison of body weights at week 12 revealed that WT females were 9% heavier than heterozygous females, whereas WT males were 14% heavier than heterozygous males (Figure 4C and D). The observed difference in weight was not related to a difference in body length, as the femur length was comparable for both females and males (Figure 4E and F). In addition, heterozygous females were less able to regulate a glucose load, whereas males were more sensitive to insulin than WT siblings (Figure 4G and H). Body composition analysis revealed that heterozygous females also had less lean content at 12 weeks, but no other differences were observed (Figure 4I–L). These results indicate that global PMCA1 haploinsufficiency affects offspring weight and metabolic parameters. The mechanism(s) underlying this phenotype are likely complex due to ubiquitous expression of PMCA1.

To determine if abnormal Ca^{2+} exposure at fertilization impacts offspring growth in genotype-matched offspring,

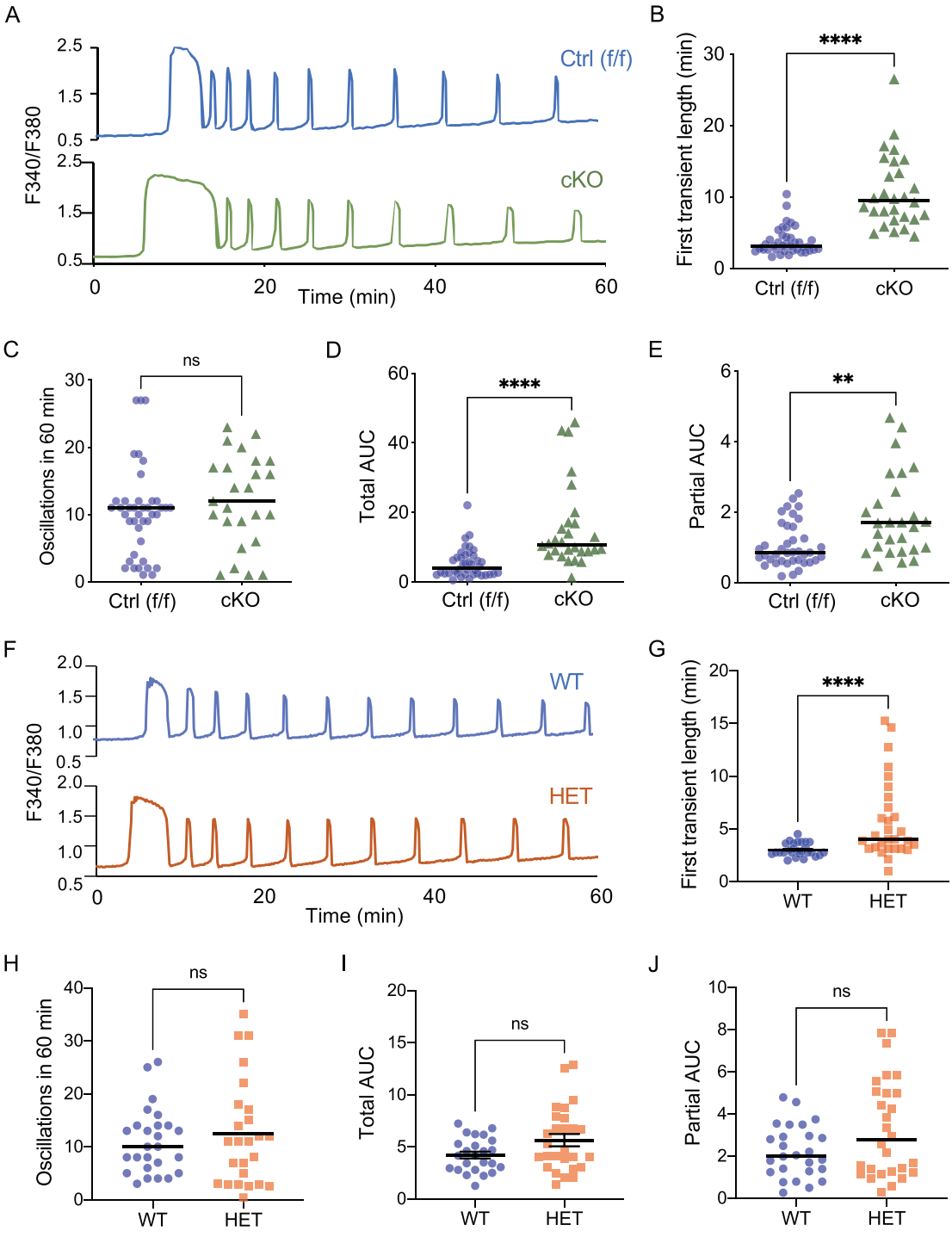

Figure 2. PMCA1 cKO eggs show aberrant Ca^{2+} responses at fertilization. (A–E) Ratiometric Ca^{2+} imaging during IVF of control (blue) and cKO (green) eggs. (F–J) Ratiometric Ca^{2+} imaging during IVF of control (blue) and heterozygous (HET, orange) eggs. N = 3 independent experiments. Each dot represents a single fertilized egg. (A, F) Representative Ca^{2+} traces. (B, G) Length in minutes of the first Ca^{2+} transient. (C, H) Number of oscillations in 60 min. (D, I) AUC for 60 min. (E, J) AUC for 60 min excluding the first transient. Mann–Whitney test; **** $p < 0.0001$; ** $p < 0.002$; ns, not significant; AUC, area under the curve.

heterozygous controls from WT dams and heterozygous offspring from cKO dams were compared. Notably, the growth of heterozygous offspring derived from cKO dams, and high Ca^{2+} at fertilization, was different than heterozygous controls derived from WT dams, and the difference was apparent by 1 week of age (Figure 5A and B). Comparison of body weights at week 12 revealed that cKO-derived females were 6% heavier than heterozygous control females, whereas cKO-derived males were 9% heavier than heterozygous control males (Figure 5C and D). Interestingly, heterozygous offspring that had high Ca^{2+} at fertilization were similar in weight to WT offspring (Figure 4C and D and Figure 5C and D). Despite the difference in weight, femur length was comparable between groups

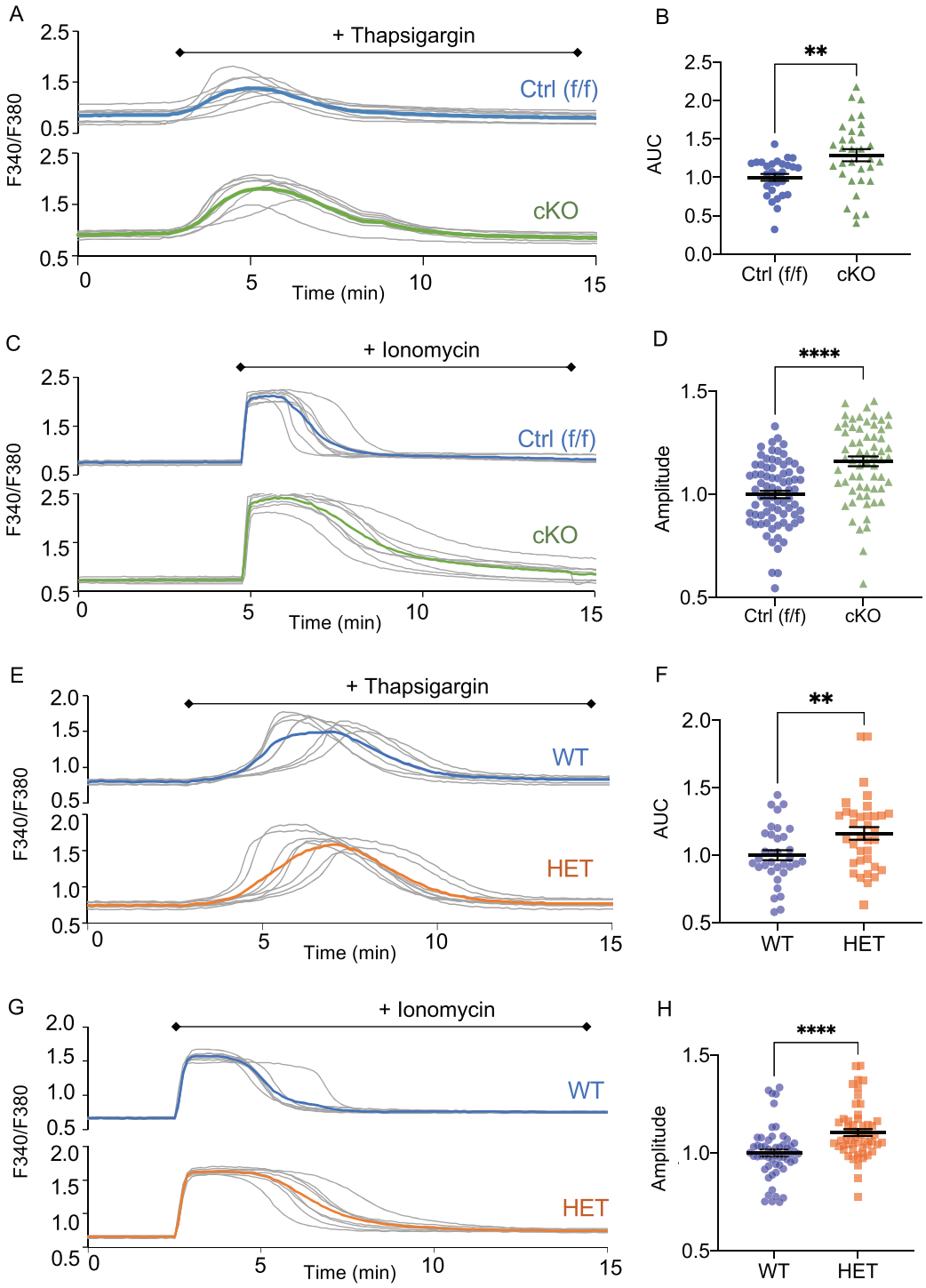

Figure 3. PMCA1 cKO eggs have increased internal Ca^{2+} stores. Measurement of Ca^{2+} stores in eggs from control (blue) and cKO (green) females (A–D) or eggs from WT (blue) and heterozygous (orange) siblings (E–H). TG was used to deplete ER Ca^{2+} stores and ionomycin was used to determine relative levels of total Ca^{2+} stored in the cell. (A, C, E, G) Representative traces are shown in color, whereas gray traces are individual measurements. (B, F) AUC following TG treatment. (D, H) Peak amplitude following ionomycin treatment. Each experiment was performed three times. Each dot represents a single egg and data are presented normalized to the control. Normally distributed data were analyzed by *t*-test (B,D,F). Otherwise, Mann–Whitney test was used (H). $^{**}p < 0.01$; $^{****}p < 0.0001$; AUC, area under the curve.

for both females and males (Figure 5E and F). These results support the idea that abnormal Ca^{2+} signaling in the first few hours following fertilization impacts offspring weight and that the weight difference cannot be explained by an impact on overall body length.

No significant differences were found in glucose tolerance or insulin tolerance, even though experimental males appeared to have lower glucose tolerance based on mean AUC (Figure 5G and H). However, comparison of body composition revealed that males, but not females, had significantly

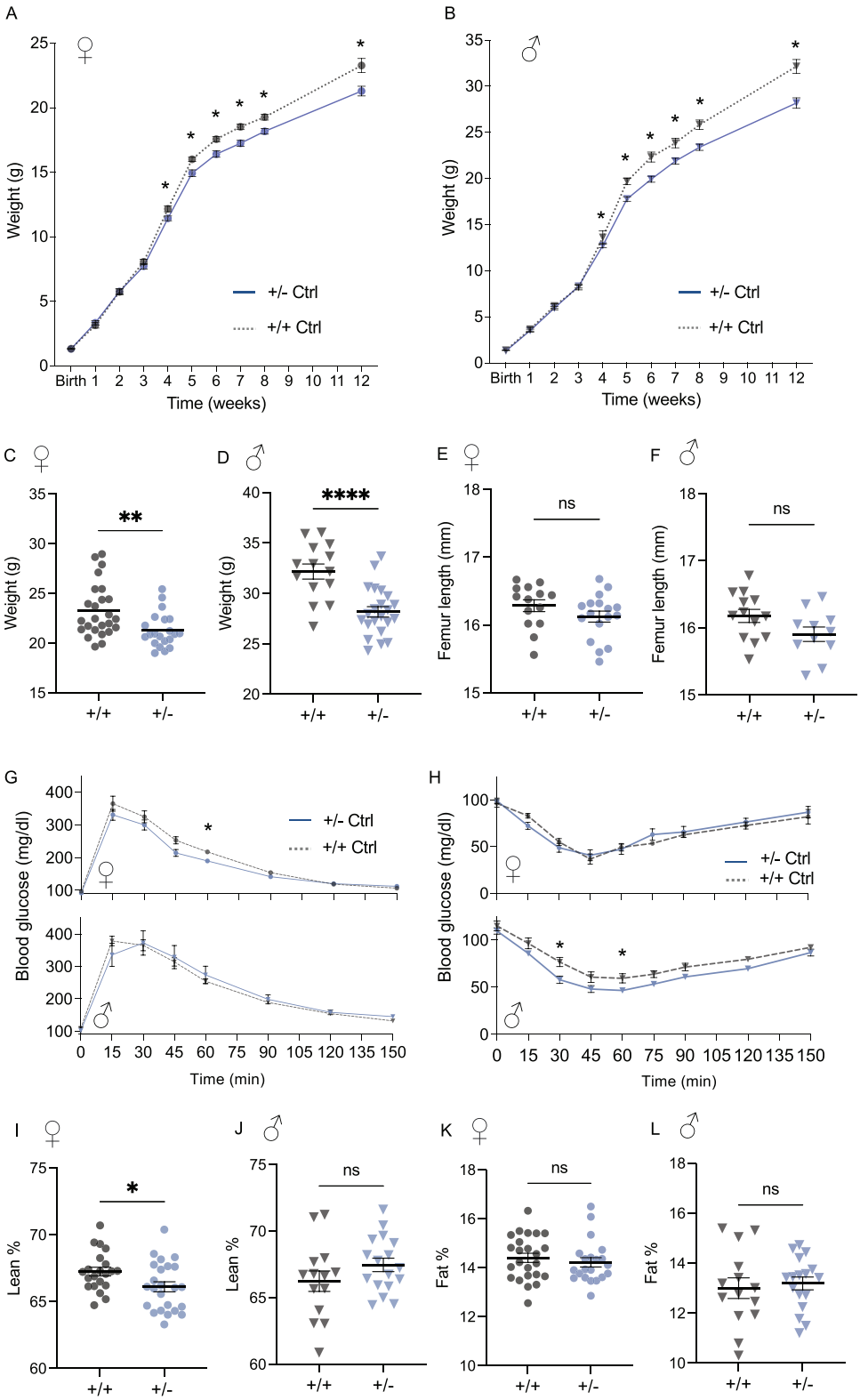

Figure 4. Global PMCA1 haploinsufficiency affects offspring weight and metabolic parameters. Growth trajectories of females (A) and males (B) shown as mean weight ± SEM over time. Offspring were obtained from WT females and heterozygous males, from 11 different dams. N = 21 heterozygous females (blue, solid line), N = 25 WT females (gray, dotted line), N = 20 heterozygous males (blue, solid line) and 14 WT males (gray, dotted line). *$p < 0.05$, uncorrected *t*-tests. (C) Female weight at 12 weeks of age. Median and all values shown. **$p < 0.005$, Mann–Whitney test. (D) Male weight at 12 weeks of age. Mean ± SEM. ****$p < 0.0001$, *t*-test. (E,F) Femur length. Mean ± SEM; *t*-test; ns, not significant. (G) Glucose tolerance test and (H) insulin tolerance test; females in upper panels and males in lower panels. Mean blood glucose ± SEM over time. Linear mixed model with Šidák correction, *$p < 0.05$. (I–L) Body composition analysis. Percentage lean content (I,J) and percentage fat content (K,L). Mean ± SEM. ***$p < 0.0005$, *t*-test. ●, females; ▼, males.

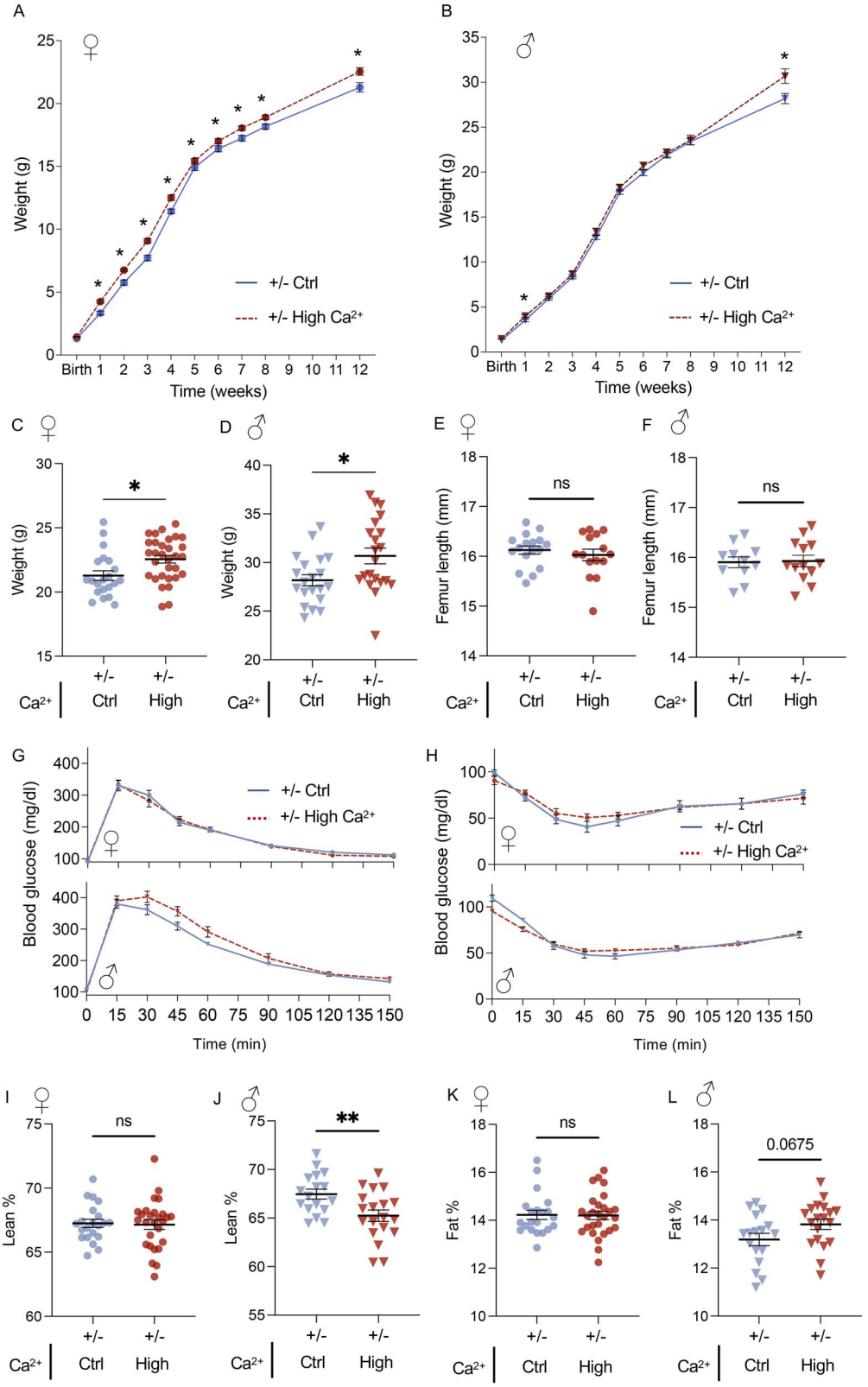

Figure 5. Abnormal Ca^{2+} at fertilization impacts offspring growth and male body composition. Growth trajectories of females (A) and males (B) shown as mean weight ± SEM over time. N = 21 heterozygous female and 20 heterozygous male pups from WT females (blue solid line, control Ca^{2+} at fertilization). N = 31 heterozygous female and 22 heterozygous male pups from cKO dams (red dashed line, high Ca^{2+} at fertilization). Pups from each genotype were obtained from at least eight different dams. *$p < 0.05$, uncorrected *t*-tests. (C,D) Weight at 12 weeks of age. Mean ± SEM. *$p < 0.02$, *t*-test. (E,F) Femur length. *t*-test; ns, not significant. (G) Glucose tolerance test and (H) insulin tolerance test; females in upper panels and males in lower panels. Mean blood glucose ± SEM over time. Linear mixed model with Šidák correction, not significantly different. (I-L) Body composition analysis. Percentage of lean content (I,J) and percentage of fat content (K,L). Mean ± SEM. **$p < 0.005$, *t*-test. •, females; ▼, males. Note that the data plotted for heterozygous offspring from WT females are the same as the data plotted in Figure 4.

less lean content and tended to have more fat (Figure 5I–L). Altogether, our results suggest that abnormal Ca^{2+} signaling at fertilization in vivo results in long-term changes in offspring growth in females and males and in body composition in males.

Discussion

Numerous in vitro studies support the notion that Ca^{2+} signaling is exceptionally important for fertilization, egg activation and proper embryo development [32, 33]. Here we generated a new genetic model of Ca^{2+} overexposure following fertilization, an oocyte-specific cKO of PMCA1, so that we could test whether this was also true when fertilization occurs in vivo, in the highly specialized environment of the oviduct. Using the PMCA1 cKO mouse model, we discovered a requisite role for PMCA1 in supporting Ca^{2+} efflux at fertilization. Second, we determined that mice globally haploinsufficient for PMCA1 (*Atp2b1*+/−) have a clear growth defect relative to their WT siblings. We were surprised by this finding because previous studies did not report differences between PMCA1 heterozygous and WT mice [20, 34] and even indicated that "PMCA1Ht mice were indistinguishable by eye from WT" [20]; however, these studies did not report any data on growth or weight. Finally, we found that heterozygous (*Atp2b1*+/−) offspring derived from cKO eggs were heavier than genotype-matched offspring derived from control eggs and that the heterozygous males from cKO eggs had less lean content than heterozygous controls. Our results indicate that abnormal Ca^{2+} signaling at fertilization in vivo has a long-term impact on offspring weight and body composition.

By comparing the Ca^{2+} dynamics of cKO and control eggs at fertilization, we determined that PMCA1 clearly functions in Ca^{2+} homeostasis at fertilization by supporting the reduction in cytoplasmic Ca^{2+} levels following each Ca^{2+} transient. This finding was most obvious in the 3-fold increase in the length of the first transient, but also was observed as an ongoing impact on the subsequent transients. However, even without PMCA1, the cytoplasmic Ca^{2+} levels returned to baseline after each transient, indicating that other mechanisms that support Ca^{2+} reuptake and efflux are operational in eggs. These additional mediators likely include SERCA2B, which supports Ca^{2+} reuptake into the ER [19], and PMCA3, which we showed was expressed in mouse oocytes at the RNA level (Figure 1). Although mitochondrial Ca^{2+} uptake occurs during egg activation [35] and, in principle, could affect cytoplasmic Ca^{2+} levels, it is not clear that the amount of Ca^{2+} that enters the mitochondria significantly impacts the overall cytoplasmic Ca^{2+} level in any way other than its impact on generation of ATP, which is essential for both SERCA and PMCA function.

Although PMCA1 cKO eggs had more total Ca^{2+} exposure at fertilization than controls, cKO females were fertile and had normal litter sizes. It was previously shown that mouse eggs can tolerate an overdose of Ca^{2+} during or after egg activation [5, 6]. Both freshly ovulated eggs and fertilized eggs (1C embryos) exposed to high Ca^{2+} levels in vitro efficiently activate as indicated by pronuclear formation, blastocyst development, and implantation. However, in contrast to our in vivo model, fertilized eggs exposed to high Ca^{2+} in vitro resulted in lower development to term after embryo transfer [6]. It is possible that the difference in developmental potential in these two models is due to a difference in the total Ca^{2+} exposure. A rough estimation suggests that the Ca^{2+} overdose treatment utilized by Ozil et al. [6] (20 electropermeabilization pulses in 40 min) results in 300% more Ca^{2+} exposure in the first hour than controls, which is about four times more Ca^{2+} than our in vivo model. Because eggs integrate the Ca^{2+} signal over time [5], a 4-fold difference in total Ca^{2+} exposure could explain the more dramatic phenotype reported. Moreover, electropermeabilization increases cytoplasmic Ca^{2+} by allowing extracellular Ca^{2+} to enter the cell, so spatial information normally encoded in IP_3 receptor-mediated Ca^{2+} release is lost in the in vitro model. Besides extracellular Ca^{2+}, other components of the culture medium such as antibiotics, lactate, pyruvate or glucose could pass through the temporary pores into the egg cytosol and contribute to metabolic disruption. Results of our experiments demonstrate that PMCA1 is important for Ca^{2+} homeostasis at fertilization and that eggs can tolerate at least a 65% increase in Ca^{2+} exposure at fertilization in vivo with no compromise in developmental competence necessary to support live birth. It remains unclear what is the maximum amount of Ca^{2+} eggs can tolerate at fertilization in vivo before development to term is affected.

An important finding from our experiments is that excess Ca^{2+} at fertilization in vivo appears to impact postnatal growth and offspring weight. Previous studies reported compelling evidence of a long-term impact of abnormal Ca^{2+} signaling after fertilization in vitro. By using electropermeabilization, Ozil et al. [6] demonstrated that fertilized eggs exposed to an excess Ca^{2+} signal have lower body weight than controls. In contrast, when Ca^{2+} signals were manipulated to be subnormal, implantation was impaired but postnatal growth was unaffected. Although these in vitro studies were revealing, it is unclear if the outcomes reported resulted from the combined effects of in vitro manipulation and altered Ca^{2+} signaling, or were a consequence of altered Ca^{2+} signaling alone. We previously demonstrated that subnormal Ca^{2+} exposure in vivo impacts offspring growth trajectory using a mouse model in which eggs lacked TRPM7 (transient receptor potential cation channel subfamily M member 7) and $Ca_V3.2$, two Ca^{2+} channels responsible for Ca^{2+} influx at fertilization. Lack of these channels in eggs dramatically diminishes total Ca^{2+} signal at fertilization and causes subfertility and alterations in postnatal weight variability [16]. It is likely that the Ca^{2+} threshold needed for proper embryo development is not reached in these eggs, interfering with proper postnatal growth. Our results expand the understanding of the importance of Ca^{2+} homeostasis at fertilization by demonstrating that not only subnormal Ca^{2+} exposure in vivo, but also excess Ca^{2+} signaling in vivo, impacts postnatal offspring growth and body composition.

It is possible that factors other than altered Ca^{2+} in the egg following fertilization could have influenced offspring weight. A well-established contributor to offspring weight is differences in litter size. It is highly unlikely that litter size could have affected our results because the sizes were not significantly different, the pup birth weights were not different, and all litters were standardized to eight pups. Another potential contributor to the weight differences is differences in the epigenetic payload of sperm derived from heterozygous PMCA1 males, which we demonstrated weighed less than WT males. For example, differences in sperm epigenetic marks or differences in small RNAs that enter the egg with sperm-egg fusion can impact offspring metabolism [36–38]. Unfortunately, testing this idea is not possible with

the genetic models we generated. Offspring from matings of heterozygous females to WT males could be tested for weight differences; however, the longer first Ca^{2+} transient observed in the eggs from these females would make these results difficult to interpret. Although we cannot rule out some impact of epigenetic differences in the sperm, we do not believe that this is the primary reason for the weight differences observed. The clear experimental differences in Ca^{2+} signaling, combined with previous findings regarding Ca^{2+} signals influencing growth when Ca^{2+} was manipulated in vitro, lead us to conclude that the differences are most likely due to the altered Ca^{2+} signaling at fertilization.

The developmental origins of health and disease (DOHaD) hypothesis proposes that there is a link between in utero exposure to environmental stressors and permanent alterations observed in offspring physiology [39]. Our data regarding the long-term impact of abnormal Ca^{2+} signaling at fertilization in vivo support previous evidence that DOHaD can be "extrapolated back" to the fertilization period [6, 40]. From this perspective, our findings are particularly relevant for environmental conditions that affect the egg's ability to handle Ca^{2+}. Ca^{2+} oscillation patterns can be modified in vitro by changing the ionic composition of culture media, such as in assisted reproduction [7, 16, 41]. Indeed, a variety of culture conditions are used by different practitioners of both domestic animal and human assisted reproduction. Concentrations of Ca^{2+} and magnesium, which are critical for proper Ca^{2+} signaling at fertilization, vary widely among commercially available culture media [42, 43]. Moreover, ionomycin treatment is used in some human clinical settings to induce a dramatic rise in the cytoplasmic Ca^{2+} level and promote egg activation after intracytoplasmic sperm injection [44, 45]. Although an improvement in development to term after ionomycin use is reported, it remains unclear if this treatment has negative long-term effects on offspring physiology.

In addition to in vitro manipulation, Ca^{2+} dynamics could be altered by mutations in Ca^{2+} modulators or conditions affecting mitochondrial function [46]. For example, numerous mutations in the *ATP2B1* sequence have been identified in humans, including one loss of function and 271 missense mutations (Genome Aggregation Database browser at gnomad.broadinstitute.org). Interestingly, a single nucleotide polymorphism in maternal *ATP2B1* is associated with higher risk of preeclampsia and low birth weight [47]. This finding could be explained by a role for PMCA1 in placental function [48]; however, a contribution of abnormal Ca^{2+} signaling during egg activation to this phenotype cannot be ruled out. Moreover, Ca^{2+} oscillations can be altered by obesity and inflammation through their impact on redox balance and mitochondrial function [46, 49]. Our results raise awareness of the importance of appropriate Ca^{2+} signaling at fertilization to ensure proper offspring growth and health.

Supplementary material

Supplementary material is available at *BIOLRE* online.

Author contributions

V.S. and C.J.W. designed the study. V.S. and P.S. conducted the experiments. V.S. and M.S. analyzed the data. V.S. wrote the first draft of the manuscript. V.S., P.S., M.S. and C.J.W. edited the manuscript.

Data availability

The data underlying this article will be shared on reasonable request to the corresponding author.

Acknowledgements

We thank Gary Bird and Xiaoling Li (NIEHS) for critical review of the manuscript.

Conflict of interest

The authors have no conflicts of interest to declare.

References

1. Ducibella T, Huneau D, Angelichio E, Xu Z, Schultz RM, Kopf GS, Fissore R, Madoux S, Ozil JP. Egg-to-embryo transition is driven by differential responses to Ca 2+ oscillation number. *Dev Biol* 2002; **250**:280–291.
2. Markoulaki S, Matson S, Ducibella T. Fertilization stimulates long-lasting oscillations of CaMKII activity in mouse eggs. *Dev Biol* 2004; **272**:15–25.
3. Backs J, Stein P, Backs T, Duncan FE, Grueter CE, McAnally J, Qi X, Schultz RM, Olson EN. The gamma isoform of CaM kinase II controls mouse egg activation by regulating cell cycle resumption. *Proc Natl Acad Sci U S A* 2010; **107**:81–86.
4. Knott JG, Gardner AJ, Madgwick S, Jones KT, Williams CJ, Schultz RM. Calmodulin-dependent protein kinase II triggers mouse egg activation and embryo development in the absence of Ca2+ oscillations. *Dev Biol* 2006; **296**:388–395.
5. Toth S, Huneau D, Banrezes B, Ozil JP. Egg activation is the result of calcium signal summation in the mouse. *Reproduction* 2006; **131**:27–34.
6. Ozil JP, Banrezes B, Toth S, Pan H, Schultz RM. Ca2+ oscillatory pattern in fertilized mouse eggs affects gene expression and development to term. *Dev Biol* 2006; **300**:534–544.
7. Ozil JP, Sainte-Beuve T, Banrezes B. [Mg2+]o/[Ca2+]o determines Ca2+ response at fertilization: tuning of adult phenotype? *Reproduction* 2017; **154**:675–693.
8. Lira-Albarran S, Liu X, Lee SH, Rinaudo P. DNA methylation profile of liver of mice conceived by in vitro fertilization. *J Dev Orig Health Dis* 2022; **13**:358–366.
9. Sandovici I, Fernandez-Twinn DS, Hufnagel A, Constancia M, Ozanne SE. Sex differences in the intergenerational inheritance of metabolic traits. *Nat Metab* 2022; **4**:507–523.
10. Rivera RM, Stein P, Weaver JR, Mager J, Schultz RM, Bartolomei MS. Manipulations of mouse embryos prior to implantation result in aberrant expression of imprinted genes on day 9.5 of development. *Hum Mol Genet* 2008; **17**:1–14.
11. Li Y, Tribulo P, Bakhtiarizadeh MR, Siqueira LG, Ji T, Rivera RM, Hansen PJ. Conditions of embryo culture from days 5 to 7 of development alter the DNA methylome of the bovine fetus at day 86 of gestation. *J Assist Reprod Genet* 2020; **37**:417–426.
12. Mehlmann LM, Kline D. Regulation of intracellular calcium in the mouse egg: calcium release in response to sperm or inositol trisphosphate is enhanced after meiotic maturation. *Biol Reprod* 1994; **51**:1088–1098.
13. Kline D, Kline JT. Thapsigargin activates a calcium influx pathway in the unfertilized mouse egg and suppresses repetitive calcium transients in the fertilized egg. *J Biol Chem* 1992; **267**:17624–17630.
14. Igusa Y, Miyazaki S. Effects of altered extracellular and intracellular calcium concentration on hyperpolarizing responses of the hamster egg. *J Physiol* 1983; **340**:611–632.
15. Bernhardt ML, Zhang Y, Erxleben CF, Padilla-Banks E, McDonough CE, Miao YL, Armstrong DL, Williams CJ. CaV3.2 T-type channels mediate Ca(2)(+) entry during oocyte maturation and following fertilization. *J Cell Sci* 2015; **128**:4442–4452.

16. Bernhardt ML, Stein P, Carvacho I, Krapp C, Ardestani G, Mehregan A, Umbach DM, Bartolomei MS, Fissore RA, Williams CJ. TRPM7 and CaV3.2 channels mediate Ca(2+) influx required for egg activation at fertilization. *Proc Natl Acad Sci U S A* 2018; **115**:E10370–E10378.
17. El-Jouni W, Jang B, Haun S, Machaca K. Calcium signaling differentiation during Xenopus oocyte maturation. *Dev Biol* 2005; **288**: 514–525.
18. Miao YL, Stein P, Jefferson WN, Padilla-Banks E, Williams CJ. Calcium influx-mediated signaling is required for complete mouse egg activation. *Proc Natl Acad Sci U S A* 2012; **109**:4169–4174.
19. Wakai T, Zhang N, Vangheluwe P, Fissore RA. Regulation of endoplasmic reticulum Ca(2+) oscillations in mammalian eggs. *J Cell Sci* 2013; **126**:5714–5724.
20. Okunade GW, Miller ML, Pyne GJ, Sutliff RL, O'Connor KT, Neumann JC, Andringa A, Miller DA, Prasad V, Doetschman T, Paul RJ, Shull GE. Targeted ablation of plasma membrane Ca2+-ATPase (PMCA) 1 and 4 indicates a major housekeeping function for PMCA1 and a critical role in hyperactivated sperm motility and male fertility for PMCA4. *J Biol Chem* 2004; **279**:33742–33750.
21. Chen J, Sitsel A, Benoy V, Sepulveda MR, Vangheluwe P. Primary active Ca(2+) transport systems in health and disease. *Cold Spring Harb Perspect Biol* 2020; **12**:a035113.
22. Zacharias DA, Kappen C. Developmental expression of the four plasma membrane calcium ATPase (Pmca) genes in the mouse. *Biochim Biophys Acta* 1999; **1428**:397–405.
23. de Vries WN, Binns LT, Fancher KS, Dean J, Moore R, Kemler R, Knowles BB. Expression of Cre recombinase in mouse oocytes: a means to study maternal effect genes. *Genesis* 2000; **26**:110–112.
24. Skarnes WC, Rosen B, West AP, Koutsourakis M, Bushell W, Iyer V, Mujica AO, Thomas M, Harrow J, Cox T, Jackson D, Severin J *et al.* A conditional knockout resource for the genome-wide study of mouse gene function. *Nature* 2011; **474**:337–342.
25. Savy V, Stein P, Shi M, Williams CJ. Superovulation does not alter calcium oscillations following fertilization. *Front Cell Dev Biol* 2021; **9**:762057.
26. Chatot CL, Ziomek CA, Bavister BD, Lewis JL, Torres I. An improved culture medium supports development of random-bred 1-cell mouse embryos in vitro. *J Reprod Fertil* 1989; **86**:679–688.
27. Jefferson WN, Chevalier DM, Phelps JY, Cantor AM, Padilla-Banks E, Newbold RR, Archer TK, Kinyamu HK, Williams CJ. Persistently altered epigenetic marks in the mouse uterus after neonatal estrogen exposure. *Mol Endocrinol* 2013; **27**:1666–1677.
28. Pfaffl MW. A new mathematical model for relative quantification in real-time RT-PCR. *Nucleic Acids Res* 2001; **29**:e45.
29. Schultz RM, Stein P, Svoboda P. The oocyte-to-embryo transition in mouse: past, present, and future. *Biol Reprod* 2018; **99**: 160–174.
30. Tatsuki F, Sunagawa GA, Shi S, Susaki EA, Yukinaga H, Perrin D, Sumiyama K, Ukai-Tadenuma M, Fujishima H, Ohno R, Tone D, Ode KL *et al.* Involvement of Ca(2+)-dependent hyperpolarization in sleep duration in mammals. *Neuron* 2016; **90**:70–85.
31. Thastrup O, Cullen PJ, Drobak BK, Hanley MR, Dawson AP. Thapsigargin, a tumor promoter, discharges intracellular Ca2+ stores by specific inhibition of the endoplasmic reticulum Ca2(+)-ATPase. *Proc Natl Acad Sci U S A* 1990; **87**:2466–2470.
32. Sanders JR, Swann K. Molecular triggers of egg activation at fertilization in mammals. *Reproduction* 2016; **152**:R41–R50.
33. Stein P, Savy V, Williams AM, Williams CJ. Modulators of calcium signalling at fertilization. *Open Biol* 2020; **10**:200118.
34. Little R, Zi M, Hammad SK, Nguyen L, Njegic A, Kurusamy S, Prehar S, Armesilla AL, Neyses L, Austin C, Cartwright EJ. Reduced expression of PMCA1 is associated with increased blood pressure with age which is preceded by remodelling of resistance arteries. *Aging Cell* 2017; **16**:1104–1113.
35. Dumollard R, Marangos P, Fitzharris G, Swann K, Duchen M, Carroll J. Sperm-triggered [Ca2+] oscillations and Ca2+ homeostasis in the mouse egg have an absolute requirement for mitochondrial ATP production. *Development* 2004; **131**:3057–3067.
36. Hocher B, Lu YP, Reichetzeder C, Zhang X, Tsuprykov O, Rahnenfuhrer J, Xie L, Li J, Hu L, Kramer BK, Hasan AA. Paternal eNOS deficiency in mice affects glucose homeostasis and liver glycogen in male offspring without inheritance of eNOS deficiency itself. *Diabetologia* 2022; **65**:1222–1236.
37. Chen Q, Yan W, Duan E. Epigenetic inheritance of acquired traits through sperm RNAs and sperm RNA modifications. *Nat Rev Genet* 2016; **17**:733–743.
38. Rando OJ, Simmons RA. I'm eating for two: parental dietary effects on offspring metabolism. *Cell* 2015; **161**:93–105.
39. Barker DJ. The fetal and infant origins of adult disease. *Br Med J* 1990; **301**:1111.
40. Banrezes B, Sainte-Beuve T, Canon E, Schultz RM, Cancela J, Ozil JP. Adult body weight is programmed by a redox-regulated and energy-dependent process during the pronuclear stage in mouse. *PLoS One* 2011; **6**:e29388.
41. Mehregan A, Ardestani G, Akizawa H, Carvacho I, Fissore R. Deletion of TRPV3 and CaV3.2 T-type channels in mice undermines fertility and Ca2+ homeostasis in oocytes and eggs. *J Cell Sci* 2021; **134**:jcs257956.
42. Morbeck DE, Baumann NA, Oglesbee D. Composition of single-step media used for human embryo culture. *Fertil Steril* 2017; **107**:1055, e1051–1060.
43. Morbeck DE, Krisher RL, Herrick JR, Baumann NA, Matern D, Moyer T. Composition of commercial media used for human embryo culture. *Fertil Steril* 2014; **102**:759, e759–766.
44. Nikiforaki D, Vanden Meerschaut F, de Roo C, Lu Y, Ferrer-Buitrago M, de Sutter P, Heindryckx B. Effect of two assisted oocyte activation protocols used to overcome fertilization failure on the activation potential and calcium releasing pattern. *Fertil Steril* 2016; **105**:798, e792–806.
45. Miller N, Biron-Shental T, Sukenik-Halevy R, Klement AH, Sharony R, Berkovitz A. Oocyte activation by calcium ionophore and congenital birth defects: a retrospective cohort study. *Fertil Steril* 2016; **106**:590–596.
46. Liu L, Hammar K, Smith PJ, Inoue S, Keefe DL. Mitochondrial modulation of calcium signaling at the initiation of development. *Cell Calcium* 2001; **30**:423–433.
47. Wan JP, Wang H, Li CZ, Zhao H, You L, Shi DH, Sun XH, Lv H, Wang F, Wen ZQ, Wang XT, Chen ZJ. The common single-nucleotide polymorphism rs2681472 is associated with early-onset preeclampsia in Northern Han Chinese women. *Reprod Sci* 2014; **21**:1423–1427.
48. Moreau R, Daoud G, Masse A, Simoneau L, Lafond J. Expression and role of calcium-ATPase pump and sodium-calcium exchanger in differentiated trophoblasts from human term placenta. *Mol Reprod Dev* 2003; **65**:283–288.
49. Zhang L, Wang Z, Lu T, Meng L, Luo Y, Fu X, Hou Y. Mitochondrial Ca(2+) overload leads to mitochondrial oxidative stress and delayed meiotic resumption in mouse oocytes. *Front Cell Dev Biol* 2020; **8**:580876.